Computational Materials Science 171 (2020) 109085

Contents lists available at ScienceDirect

Computational Materials Science

journal homepage: www.elsevier.com/locate/commatsci

Multiphase field modelling of alloy solidification

P.C. Bollada*, P.K. Jimack, A.M. Mullis

University of Leeds, United Kingdom

ARTICLE INFO

Keywords:
Multiphase field
Alloy solidification
Crystal growth

ABSTRACT

We present an approach to alloy solidification modelling that incorporates binary interface energies in a manner that correctly reproduces the associated theoretical angles at triple junctions in eutectic solidification. We find that simply applying the principle that the correct binary junction behaviour is recovered when only two phases are present is insufficient. Previous research (Toth, 2016) recommends a modification of the surface energy by adding an energy barrier at the triple junction, and we explore alternative models that would benefit from this approach. The main approach we recommend here, though, is to extend the minimal model of Folch and Plapp (2003, 2005), which, without modification, is limited to 120° junction angles. This is achieved by a linear transformation of this formulation, and facilitated by an analytical multiphase solution presented here for the first time.

1. Notation

We begin with a short section to establish the notation.

1.1. Single phase formulation and notation

A phase field model for binary alloy solidification uses three field variables: the phase, ϕ; the concentration, c; and temperature, T. The phase field is designed to vary smoothly in the region $\phi \in [0, 1]$, where $\phi = 0$ is liquid and $\phi = 1$ is solid, and similarly the alloy component of one species varies in the range $c \in [0, 1]$. Values of ϕ away from the bulk extremes indicates a transition region lying in a smoothed out representation of the interface.

Once the variables are given, the free energy, F in terms of a free energy density, f, is constructed. This typically does not contain gradients of c or T, but it must contain gradients of ϕ to keep the interface smooth:

$$F = \int_\Omega f(\nabla\phi, \phi, c, T)\mathrm{dxdy} \tag{1}$$

where we choose without loss of generality a two dimensional domain, Ω. Evolution of ϕ is then prescribed by

$$\dot{\phi} = -M\frac{\delta F}{\delta \phi}, \tag{2}$$

where the mobility, M, is prescribed, for example as in [4], where it may be a function of c. The concentration equation

$$\dot{c} = \nabla\cdot D\nabla\frac{\delta F}{\delta c} \tag{3}$$

preserves the mass of each species and introduces the solute diffusivity, D, which is usually of the form $D = c(1-c)[(1-\phi)D_{\mathrm{liq}} + \phi D_{\mathrm{sol}}]/(RT)$ with $D_{\mathrm{sol}} \ll D_{\mathrm{liq}}$, where R is the molar gas constant.

The most complete temperature formulation was established in [5], with the simplest approximation to formulation found there being

$$C_p\dot{T} = \nabla\cdot\kappa\nabla T + L\dot{\phi} \tag{4}$$

with latent heat of fusion, L, heat capacity, C_p, and thermal conductivity, κ, are constant. In this form the heat generated by solidification ($\dot{\phi} > 0$) is clearly seen.

The free energy density may be split into two contributions: surface free energy density, $f_S(\nabla\phi, \phi)$ (and perhaps also a function of c and T), and bulk free energy density, $f_B(\phi, c, T)$:

$$f = f_S + f_B. \tag{5}$$

Crucially, the surface free energy density, f_S, is a function of gradients of ϕ and is formed such that this term vanishes in the bulk ($\phi = 0, 1$). The formulation of f_S given in [4] is of the form

$$f_S = \frac{1}{2}\epsilon^2\,\nabla\phi\cdot\nabla\phi + W\phi^2(1-\phi)^2 \tag{6}$$

where $\epsilon^2 = 6\sigma\delta$, $W = 12\sigma/\delta$, σ is the liquid-solid interfacial energy, and thus $\epsilon^2/W = \frac{1}{2}\delta^2$. Here δ has the dimensions of length and can be taken as the interface width.

The bulk energy, f_B, can be formed by combining free energy densities for each phase, $f_{\mathrm{liq}}(c, T)$ and $f_{\mathrm{sol}}(c, T)$, with the phase, ϕ, serving as a weight to interpolate between the two as will be discussed in more detail in this paper. f_{liq} and f_{sol} may be obtained from a database or

* Corresponding author.
E-mail address: p.c.bollada@leeds.ac.uk (P.C. Bollada).

https://doi.org/10.1016/j.commatsci.2019.109085
Received 11 March 2019; Received in revised form 13 June 2019; Accepted 14 June 2019

Table 1
The notational differences between single and multiphase quantities. The single index is associated with the bulk and the double indices are associated with the interface.

Physical quantity	Single phase	Multi phase
Phase	ϕ	ϕ_i, $i \in [1, n]$
Mobility	M	M_{ij}, $i, j \in [1, n]$
Energy per length	ϵ^2	ϵ_{ij}^2, $i, j \in [1, n]$
Energy height	W	W_{ij}, $i, j \in [1, n]$
Interface width	δ	δ_{ij}, $i, j \in [1, n]$
Interfacial energy	σ	σ_{ij}, $i, j \in [1, n]$
Bulk Energies	$f_{\text{liq}}, f_{\text{sol}}$	f_i, $i \in [1, n]$
Surface energy density	$f_S(\nabla\phi, \phi)$	$f_S(\nabla\bar{\phi}, \bar{\phi})$, where $\bar{\phi} = [\phi_1, \phi_2, ..., \phi_n]$

CALPHAD calculation.

1.2. To multiphase notation

To generalise the single phase formulation to an n-phase multiphase system involves defining the slightly richer notation in Table 1: All double index quantities are symmetric and there is a constraint on the phases, ϕ_i, such that $\sum_{i=1}^{n} \phi_i = 1$. Other multiphase models which do not impose this constraint will be considered in Section 4.2.

2. Motivation

We now present the current state of multiphase modelling of alloy solidification in an attempt to extract a definitive model. We build upon the prior work of [6] which lays out a series of formal constraints on the form such a model must have. For example, clearly one measure of success in any postulated multiphase model is that it must reduce to an accepted single phase model when only two phases (the solid and the melt) are present in some spatial region. Similarly [1] investigates models with respect to the reproduction of the theoretically correct angles associated with interface energy terms, W_{ij} (as well as aspects of flow, which are outside the scope of this paper). The model advocated by [6,1] incorporates interface energy into the model by creating scalar (non indexed) functions, W, of W_{ij} (and also with ϵ^2 and ϵ_{ij}^2) and the phases, ϕ_i in the following manner

$$W(\bar{\phi}) = \frac{\sum_{i<j} W_{ij}\phi_i^2\phi_j^2}{\sum_{i<j} \phi_i^2\phi_j^2} \tag{7}$$

(here $\sum_{i<j}$ means the double sum, $\sum_{j=2}^{n}\sum_{i=1}^{j-1}$), where it can be verified that when, for example, $\phi_1 + \phi_2 = 1$ we have $W = W_{12}$. In addition, for $n = 3$ phases, the energy is supplemented by a function that vanishes in the bulk and on a binary interface, $\bar{h} = |\phi_1||\phi_2||\phi_3|$. It is this combination that appears to allow energy preference to select the particular angle at triple junctions associated with the three binary values, W_{ij}. We observe, in addition to the expression Eq. (7) not being well defined in the bulk (e.g. $\phi_1 = 1$), that there may be more computation than is perhaps necessary in their proposed formulation, following the variational procedure:

$$\frac{\delta F}{\delta \phi_i} = -\nabla\cdot\frac{\partial f}{\partial \nabla\phi_i} + \frac{\partial f}{\partial \phi_i} \tag{8}$$

when f contains this term (this formulation will be stated later in this paper). How much weight to give to $\bar{h}$ in the formulation and what the generalisation is to n phases is also not rigorously established.

There is another strong motive to our paper, and this is that although much effort has been made in seeking a proper multiphase generalisation of the quartic potential well, $\phi^2(1-\phi)^2$, used in single phase, there has been a less cohesive effort in generalising the (companion) gradient term, $\nabla\phi\cdot\nabla\phi$. As we will see, there are a number of attempts to generalise this term, but, unlike the double well potentials on offer, there would appear to be no way of comparing them. We introduce a way of visualising and comparing rival gradient terms over a simplex in this paper.

3. Background

There are two main ingredients to modelling alloy solidification under the principle of energy minimisation: the diffusion parameters; and the free energy specification. Under single phase growth the mobility is the diffusion parameter associated with phase change, and, for alloys, there is an additional solute diffusion parameter associated with solute diffusion. For multiphase and/or multi-component systems these diffusion parameters become matrices. But here is the central problem in generalising from single phase to multiphase or multi-component: in single phase one variable represents a combination of two states. That is, a single phase variable, $\phi \in [0, 1]$ has at its extreme values, two states of matter (the same issue arises with the generalisation of binary alloy concentration, c). So the question arises: do we adopt variables for each bulk phase, ϕ_i, or instead choose variables representing transitions between two phases of matter, ϕ_{ij}. The latter would appear to be more closely associated with the single phase modelling, and yet the former, ϕ_i, is almost universally adopted. This causes a mismatch between physically derived quantities such as surface energies and mobilities, which are intrinsically binary in origin, and the chosen single index variables of the model, e.g. ϕ_i. The most reliable guide to forming a consistent multiphase model is that when we set $\phi_1 + \phi_2 = 1$ the system reproduces the single phase model. Inevitably, there are a number of possible multiphase models that have this feature.

Let us assume that given M_{ij} and W_{ij} a multiphase model reduces correctly to the single phase model, then this implies that the equations for ϕ_i and ϕ_j cannot depend on any other indices except i, j. That is, for $(i, j) = (1, 2)$ there can only be dependency on ϕ_1, ϕ_2 and also W_{12} (it can, however, depend on M_{11}, M_{22}, M_{12} and M_{21}).

An ideal multiphase model has a double index dependence (or more) in the surface energy and single index dependence in bulk behaviour. Thus given database energy density functions, $f_i(c, T)$ for each phase, ϕ_i, we might form the bulk energy as

$$f_B = \sum_i g(\phi_i) f_i \tag{9}$$

where g is some monotonic function that interpolates between 0 and 1. Yet, even in this relatively simple term, Eq. (9) is incorrect: $g(\phi_i)$ cannot be set equal to ϕ_i since this results in a driving force independent of phase. Also it cannot be any other function because $\sum g(\phi_i) \neq 1$ in general. A correct interpolation could read

$$f_B = \sum_i g_i(\bar{\phi}) f_i \tag{10}$$

where g_i, such that $\sum g_i = 1$, must be a function of all phases, i.e. they must be properly constructed weights. However, there are other approaches, for example, [7,8].

The latent heat of fusion is also naturally a double index quantity, because it is associated with a transition between two phases (even potentially solid-solid). In single phase models, heat generation is associated with phase change and a term (see, for example, [9] for pure metal solidification)

$$L\dot{\phi} \tag{11}$$

but, again, it is by no means obvious how a quantity, L_{ij} can be incorporated into a multiphase model. Following a thermodynamically consistent approach developed by [10], and consistent with [11], this problem was resolved in [5], and, in fact, a single index quantity is advocated there for the heat source term.

As stated in Eq. (2), the mobility parameter, M is incorporated into a

single phase model by

$$\dot{\phi} = -M\frac{\delta F}{\delta \phi} \tag{12}$$

where F is the free energy functional. Initial attempts to generalise include

$$\dot{\phi}_i = -M\frac{\delta F}{\delta \phi_i} \tag{13}$$

but it was observed that this will not guarantee the constraint $\sum \phi_i = 1$ (see [12]), which lead to the introduction of a Lagrange multiplier approach. Looked at more generally the Lagrange multiplier approach is part of a family of formulations of the form

$$\dot{\phi}_i = -M_{ij}\frac{\delta F}{\delta \phi_j} \tag{14}$$

where, in the case of a Lagrange multiplier, the matrix M_{ij} has constant entries and guarantees that $\sum \dot{\phi}_i = 0$. This formulation correctly reduces to single phase, but [13] formally recognised and resolved, a fact well known in the modelling community, that this model exhibits n phase dependence. This is the disadvantageous modelling trait that on any n-junction, other phases play a part in the dynamics (other that the n phases present).

Perhaps unique in multiphase modelling is the model advocated by [14]. This model is n-phase independent and exhibits a model construction that incorporates double index quantities naturally. The formal objection to the model is that it does not construct a total free energy. The model was recognised at the time by its author as having shortcomings, and more recently [6] revealed that free energy minimisation was not guaranteed. It also does not lend itself to incorporating a temperature field by the methods of [5]. That said, there seems to be no formal argument that this model is incorrect, largely due to the non-physical nature of the interface region. Furthermore, this model has significant advantage computationally since it has fewer complex terms, and does not generate spurious phases.

One critical feature of phase field modelling is the balance between gradient terms and potential terms that form the surface energy density. The premise is that a finite gradient in the transition region (phase-phase interface) evolves due to the balance of these two terms. The double well potential term is readily visualised, as it is a function of phase, and has minima at the two extremes and a maximum at the junction. Thus this term attempts to create a steep gradient between the two phases. Typically a quartic function of phase is used as being the lowest order polynomial that has zero derivatives at the extremes. In passing, it may be observed that this function has a finite second derivative which also plays a part in the dynamics of solidification. Extending this function to three phases and more is not obvious. In fact, it is our view that this term is still not optimal in models to date despite recent improvements in understanding, [6]. The problem is to construct a potential that both increases away from an n-junction towards an $(n+1)$-junction, and also incorporates the double index surface energies in a natural way. That is, the potential needs to provide a barrier to the formation of another phase from bulk; a further barrier to the formation of three phases from two, etc. The solution in [6] is to first assume equal surface energies and successfully find a polynomial that has all the right characteristics. They then combine the double index quantities into the single scalar, W, given in Eq. (7), which multiplies this function of ϕ_i. The function W has the property that it equals the average of the binary heights at the triple junction which, in general, must be lower than one of the binary heights, W_{ij}. This discrepancy can be compensated for, as shown in [1], by introducing a special triple junction term $\phi_1\phi_2\phi_3$. Although it is no doubt correct, for generality, to incorporate a triple term, such a term may also be added to other models to achieve the same effect at less computational cost, e.g. the potential in [12], $\sum_{i<j} W_{ij}\phi_i^2\phi_j^2$. The scalar functions, W, apart from being slightly complicated also suffer from the awkward feature that they are not defined in the bulk (see also [37]). The scalar functions, W, apart from being slightly complicated also suffer from the awkward feature that they are not defined in the bulk. These two facts suggest that there may yet be a more elegant solution to this problem.

Designing a potential term for more than two phases is at least readily analysable (and easily illustrated for three phases), so that one can see at a glance the changes in phase implied by the gradients. This is not the situation with the gradient energy, being a function of, at least, $\nabla\phi_i$ and possibly also ϕ_i. Perhaps because of this, rival formulations for this term have not been the subject of comparison or significant discussion. The approach of [6] to the potential term does lend itself to the postulation of the gradient term, and it certainly appears that this combination of potential and gradient energy terms is the most consistent in use today. That said, we believe there are other avenues of investigation that have not been tried. One of these is discussed here in Section 5, where we construct a multiphase solution analogous to the tanh profile 1D solution adopted in single phase modelling. Using this, we are able to inspect the gradient term as a function on the simplex (i.e. not only the potential term). The results are revealing. For example, we know that the potential term in [12] exhibits a lower triple junction energy, but, surprisingly, inspection of the gradient term used in [12] also has this feature. Also, using this visualisation, the model advocated by [6] does not appear to have the same energy shape as exhibited in their own potential. All the above seem to suggest that the optimum multiphase model has yet to be found.

One way of discussing the candidate gradient energy models is to note that they are all quadratic in gradients and so fit the general form

$$f_G = \sum_{ij} \alpha_{ij}\nabla\phi_i\cdot\nabla\phi_j \tag{15}$$

where α_{ij} can be functions of, $\bar{\phi}$ (i.e. ϕ_i, $i \in [1, n]$). Applying the principle that the multiphase model reduces to single phase when $n = 2$ appears to narrow the models found in the literature to a handful of candidates. We can also use α_{ij} to postulate new models that necessarily reduce to single phase when $n = 2$. This is compelling in itself, but we also find later in the paper, using a constructed three phase solution, further models which have extra desirable features - not least the ability to incorporate binary surface energies, σ_{ij}.

4. Multiphase field modelling

We discuss present approaches to multiphase modelling, for example, binary alloys with three distinct phases of matter represented by ϕ_1 (liquid), ϕ_2 (solid 1) and ϕ_3 (solid 2). Clearly $\sum_i^n \phi_i = 1$ where $n = 3$ in this case. As in the single phase formulation, Eq. (1), the total free energy on the domain, Ω is defined in terms of its density:

$$F = \int_\Omega f\,\mathrm{dxdy} \tag{16}$$

where, without loss of generality we assume 2 spatial dimensions (2D) in two Cartesian coordinates x, y.

Given Eq. (14), a form for M_{ij} stems from the work described in [13]:

$$M_{ij} = -M(c)\frac{\phi_i\phi_j}{(1-\phi_i)(1-\phi_j)},\ i \neq j, \tag{17}$$

with diagonal entries given by $M_{ii} = -\sum_{j\neq i} M_{ij}$ (no implied summation on the left). Eq. (17) is easily generalised to accommodate binary interface mobilities, m_{ij} by

$$M_{ij} = -M(c)\frac{m_{ij}\phi_i\phi_j}{(1-\phi_i)(1-\phi_j)},\ i \neq j. \tag{18}$$

This formulation allows, for example, kinetic anisotropy to be included into a multiphase formulation by associating an i, j anisotropy, A_{ij} with m_{ij}, but an exploration of this topic is beyond the scope of this paper.

Associated with minimisation of free energy is the optimal increase

of entropy, which can in turn be related to temperature changes. In [10] the authors advocate the application of a dissipative bracket for modelling relaxation phenomena. By applying this approach to multiphase alloy solidification [5] gives the temperature field as

$$C\dot{T} = \nabla\cdot\mathbf{j} - \left(1 - T\frac{\partial}{\partial T}\right)\frac{\delta F}{\delta \phi_i}\dot{\phi}_i - \left(1 - T\frac{\partial}{\partial T}\right)\frac{\delta F}{\delta c}\dot{c} \tag{19}$$

where heat capacity is related to the free energy density by

$$C = -T\frac{\partial^2 f}{\partial T^2} \tag{20}$$

and where, in general, the heat flux, $\mathbf{j}$, has in addition to gradient of temperature, a term of entropic nature associated with the solute field:

$$\mathbf{j} = \kappa\nabla T + D\frac{\partial f}{\partial c}\nabla\frac{\partial f}{\partial c}. \tag{21}$$

Though formally present this term can be neglected in many modelling scenarios with the simplification to Eq. (19) being:

$$C\dot{T} = \nabla\cdot\kappa\nabla T - \left(1 - T\frac{\partial}{\partial T}\right)\frac{\delta F}{\delta \phi_i}\dot{\phi}_i. \tag{22}$$

For computational simplicity all models we are aware of adopt an approximation in the last term of Eq. (22) which ignore terms in the free energy relating to the surface and use

$$\frac{\delta F}{\delta \phi_i}\dot{\phi}_i \approx \frac{\partial f_B}{\partial \phi_i}\dot{\phi}_i \tag{23}$$

where the free energy density, f only contains the bulk contribution, f_B. Of course there may well be scenarios where this approximation is not valid.

4.1. Free energy construction

The remaining modelling is done within the specification of the free energy as a function of phases, ϕ_i, concentration, c, and temperature, T. The free energy is decomposed into separate surface, f_S, and bulk, f_B, contributions

$$f = f_S + f_B. \tag{24}$$

Typically, the bulk contribution, f_B is constructed using a thermodynamic database [15] and using the phase variables, ϕ_i, to interpolate [4,16]. Other methods of constructing a phase field model from database functions are found in [17] and put in context by [7,8]. For single phase alloy models the correction for interface width effects advocated in [18–20] has been generalised to multiphase, for example in [21] for dilute alloys, but is not readily generalisable to a full thermodynamic database approach. Thus one of the motivations for adopting the type of approach advocated in [17] is that there is a degree of interface width independence built in, so the generalisation to multiphase is more readily accomplished [22–26]. An alternative to [18] that builds on [4], allows computationally convenient interface widths, and the direct use of database is found in [27] though this is not yet generalised to multiphase.

The surface energy, on the other hand, serves the double role of allowing the incorporation of surface quantities and controlling the finite interface between phases. It is safe to say that, at present, there is no concensus in modelling the surface free energy in a multiphase setting.

As suggested in [6], the surface energy, f_S, can be formed by inserting the surface terms, W, outside the interface controlling terms. Amongst the simplest ways of achieving this is to combine this idea with a form originating in [2,3], namely, as a single sum over phases:

$$f_S = W(\underline{\phi})\sum_{i=1}^{3}\left(\frac{1}{2}|\delta\nabla\phi_i|^2 + \phi_i^2(1-\phi_i)^2\right). \tag{25}$$

In [1] more work is done on the double well potential than in Eq. (25) by including a triple junction term which is designed to give a higher potential barrier for three phase coexistence.

There is a perhaps more natural way to incorporate the double index quantity, W_{ij}, into the formulation used in [28,12], given by

$$f_S = \sum_{i=2}^{n}\sum_{j=1}^{i-1} W_{ij}(\delta^2 r_{ij} + \phi_i^2\phi_j^2) \tag{26}$$

where

$$r_{ij} = \frac{1}{2}|\phi_i\nabla\phi_j - \phi_j\nabla\phi_i|^2. \tag{27}$$

More "natural" in the sense that the binary barrier heights are more directly associated with two phases. Other forms for r_{ij} are also available including [29],

$$r_{ij} = C|\nabla\phi_i - \nabla\phi_j|^2, \tag{28}$$

for some combination of constants C. Another form for this term is introduced in [30]:

$$r_{ij} = -\frac{1}{2}\nabla\phi_i\cdot\nabla\phi_j. \tag{29}$$

The gradient term Eq. (29) is more computationally convenient than Eq. (27) and appears to have no obvious drawbacks.

To illustrate the potential complications in this term, we evaluate the variational derivative:

$$\begin{aligned} -\tfrac{\delta}{\delta\phi_k}\int f_S &= \nabla\cdot\tfrac{\partial f_S}{\partial\nabla\phi_k} - \tfrac{\partial f_S}{\partial\phi_k} \\ &= \tfrac{\partial}{\partial x^a}\tfrac{\partial f_S}{\partial\phi_k^a} - \tfrac{\partial f_S}{\partial\phi_k} \end{aligned} \tag{30}$$

where x^a, $a = 1..d$ are the cartesian coordinates and

$$\phi_k^a \equiv \frac{\partial\phi_k}{\partial x^a},\ \phi_k^{ab} \equiv \frac{\partial\phi_k^{\ a}}{\partial x^b}, \tag{31}$$

We then use the chain rule

$$\frac{\partial}{\partial x^a} = \phi_i^a\frac{\partial}{\partial\phi_i} + \phi_i^{ab}\frac{\partial}{\partial\phi_i^{\ b}}, \tag{32}$$

to write

$$\frac{\partial}{\partial x^a}\frac{\partial f_S}{\partial\phi_k^a} - \frac{\partial f_S}{\partial\phi_k} = \phi_i^a\frac{\partial}{\partial\phi_i}\frac{\partial f_S}{\partial\phi_k^a} + \phi_i^{ab}\frac{\partial}{\partial\phi_i^{\ b}}\frac{\partial f_S}{\partial\phi_k^a} - \frac{\partial f_S}{\partial\phi_k}. \tag{33}$$

Applying this expression to the formulation in [28] tends to give quite large expressions when compared with [30], i.e. Eqs. (26), (29) and also Eq. (25).

To get a more general view of the possibilities for the surface energy term consider the more general quadratic form

$$f_G = \sum_{i}^{n}\sum_{j}^{n}\alpha_{ij}(\bar{\phi})\nabla\phi_i\cdot\nabla\phi_j, \tag{34}$$

where α_{ij} is, in general, a function of $\phi_1, ...,\phi_n$. Using summation notation, and comma notation for derivatives of α_{ij} we find the useful expression for implementing a variety of models:

$$\begin{aligned} -\frac{\delta F_G}{\delta\phi_k} &= 2\alpha_{ik,j}\nabla\phi_j\cdot\nabla\phi_i - \alpha_{ij,k}\nabla\phi_i\cdot\nabla\phi_j + 2\alpha_{ik}\nabla^2\phi_i = (2\alpha_{ik,j} - \alpha_{ij,k})\nabla\phi_i\cdot\nabla\phi_j \\ &\quad + 2\alpha_{ik}\nabla^2\phi_i. \end{aligned} \tag{35}$$

Returning to the expression Eq. (34), a constraint on the coefficient α_{ij} is that the formulation should reduce to single phase with only two phases present, i.e. when $\phi_n + \phi_m = 1$. From Eq. (34) set (with summation on the left side only, i.e. not over n or m which are specific values)

$$f_G \equiv \alpha_{ij}\nabla\phi_i\cdot\nabla\phi_j = \frac{\delta^2}{2}W_{nm}\nabla\phi_n\cdot\nabla\phi_n. \tag{36}$$

Using $\nabla\phi_n + \nabla\phi_m = 0$ we have a constraint on the coefficients

$$\alpha_{nn} - 2\alpha_{nm} + \alpha_{mm} = \frac{\delta^2}{2}W_{nm}. \tag{37}$$

using Eq. (37), let us check the form used in [29] (adapted from Eq. (51) on page 173 in [29])

$$f_G = \sum_i^n \sum_j^n C\delta^2 W_{ij}|\nabla\phi_i - \nabla\phi_j|^2 \tag{38}$$

Then

$$\alpha_{nn} = \sum_{i\neq n} C\delta^2 W_{ni}, \alpha_{mm} = \sum_{i\neq m} C\delta^2 W_{mi}, 2\alpha_{nm} = -2C\delta^2 W_{nm} - 2C\delta^2 W_{mn} = -4C\delta^2 W_{nm}. \tag{39}$$

So in this case

$$\alpha_{nn} - 2\alpha_{nm} + \alpha_{mm} = 6CW_{nm} + \text{otherterms}, \tag{40}$$

which shows that this form does not reduce correctly. On the other hand, for [28,30] constraint Eq. (37) is satisfied. In [28]

$$\alpha_{nn} = \sum_{i\neq n} \frac{\delta^2}{2}W_{ni}\phi_i^2 = \frac{\delta^2}{2}W_{nm}\phi_m^2, \alpha_{mm} = \sum_{i\neq m} \frac{\delta^2}{2}W_{mi}\phi_i^2 = \frac{\delta^2}{2}W_{nm}\phi_n^2, \alpha_{nm} = -\delta^2 W_{nm}\phi_n\phi_m, \tag{41}$$

since

$$\alpha_{nn} - 2\alpha_{nm} + \alpha_{mm} = \frac{\delta^2}{2}W_{nm}(\phi_m^2 + 2\phi_m\phi_n + \phi_n^2) = \frac{\delta^2}{2}W_{nm}(\phi_m + \phi_n)^2 = \frac{\delta^2}{2}W_{nm} \tag{42}$$

Similarly, for [30] we have:

$$\alpha_{nn} = \alpha_{mm} = 0, \alpha_{nm} = -\frac{\delta^2}{4}W_{nm}. \tag{43}$$

We might try to create new formulations that satisfy the constraint Eq. (37) as follows:

$$\alpha_{nn} = \sum_{i\neq n} \frac{\delta^2}{4}W_{ni}\phi_i, \alpha_{nm} = 0,\ n \neq m, \tag{44}$$

giving a form which seems like a generalisation of the form given in [2], but which incorporates double index terms naturally:

$$f_G = \sum_j^n \sum_{i\neq j} \frac{\delta^2}{2}W_{ij}\phi_j\nabla\phi_i\cdot\nabla\phi_i. \tag{45}$$

In summary, by discounting Eq. (28), there are four gradient energy candidates that satisfy the 2 phase reduction correctly. We summarise these here:

1. Used in [28,12]

$$\sum_{i=2}^n \sum_{j=1}^{i-1} \frac{1}{2}W_{ij}\delta^2|\phi_i\nabla\phi_j - \phi_j\nabla\phi_i|^2. \tag{46}$$

2. Used in [30]

$$-\sum_{i=2}^n \sum_{j=1}^{i-1} \frac{1}{2}W_{ij}\delta^2\nabla\phi_i\cdot\nabla\phi_j. \tag{47}$$

3. Advocated by [6]

$$\left(\frac{\sum_{i<j} W_{ij}\phi_i^2\phi_j^2}{\sum_{i<j}\phi_i^2\phi_j^2}\right)\sum_{i=1}^3 \frac{1}{2}\delta^2\nabla\phi_i\cdot\nabla\phi_i. \tag{48}$$

4. Introduced as a candidate here in Eq. (45)

$$\sum_{i=1}^n \sum_{j\neq i}^n \frac{1}{2}W_{ij}\phi_j\nabla\phi_i\cdot\nabla\phi_i. \tag{49}$$

4.2. Double well potential

In [12], there is a problem with the double well potential $f_{DW} = W_{ij}\phi_i^2\phi_j^2$. Although it reduces to single phase when $\phi_k = 0,\ k \neq i, j$

$$\text{single phase} \Rightarrow \phi_i^2\phi_j^2 \to \phi^2(1-\phi)^2, \tag{50}$$

which implies a barrier between the two remaining phases, it does not provide a higher barrier still (even with equal W_{ij}), at the coexistence of a higher number of phases. For example, for three phase only

$$\left[\sum_{i=2}^{n=3}\sum_{j=1}^{i-1} W_{ij}\phi_i^2\phi_j^2\right]_{\phi_1=\phi_2=\phi_3=1/3} < \left[\sum_{i=2}^{n=3}\sum_{j=1}^{i-1} W_{ij}\phi_i^2\phi_j^2\right]_{\phi_1=\phi_2=1/2}. \tag{51}$$

which is easily verified when, say, $W_{ij} = 1$. This is in contrast to the double obstacle found in [30]

$$\left[\sum_{i=2}^{n=3}\sum_{j=1}^{i-1} W_{ij}|\phi_i||\phi_j|\right]_{\phi_1=\phi_2=\phi_3=1/3} > \left[\sum_{i=2}^{n=3}\sum_{j=1}^{i-1} W_{ij}|\phi_i||\phi_j|\right]_{\phi_1=\phi_2=1/2}. \tag{52}$$

and with the single index sum

$$\left[\sum_i^n \phi_i^2(1-\phi_i)^2\right]_{\phi_1=\phi_2=\phi_3=1/3} > \left[\sum_i^n \phi_i^2(1-\phi_i)^2\right]_{\phi_1=\phi_2=1/2}. \tag{53}$$

Toth et al. [6], present a more general (n phase) double well potential,

$$\frac{1}{12} + \sum_{i=1}^n \left(\frac{\phi_i^4}{4} - \frac{\phi_i^3}{3}\right) + \frac{1}{2}\sum_{i<j}\phi_i^2\phi_j^2 \tag{54}$$

which has the practical feature that higher order junctions have a higher barrier height, but combining this directly with the binary junction height, W_{ij} is not possible (due to the single index sum). So [6] postulate, in common with their treatment of the gradient term,

$$f_{DW} = \left(\frac{\sum_{i<j} W_{ij}\phi_i^2\phi_j^2}{\sum_{i<j}\phi_i^2\phi_j^2}\right)\left[\frac{1}{12} + \sum_{i=1}^n \left(\frac{\phi_i^4}{4} - \frac{\phi_i^3}{3}\right) + \frac{1}{2}\sum_{i<j}\phi_i^2\phi_j^2\right]. \tag{55}$$

For $n = 3$ phases this is identical to the simpler (which can be verified by setting $\phi_3 = 1 - \phi_1 - \phi_2$ in both cases):

$$f_{DW} = \left(\frac{\sum_{i<j} W_{ij}\phi_i^2\phi_j^2}{\sum_{i<j}\phi_i^2\phi_j^2}\right)\frac{1}{2}\sum_i \phi_i^2(1-\phi_i)^2. \tag{56}$$

In Fig. 1 we present a generalised double well potential, f_{DW}, that retains zero derivatives normal to the boundary as well as allowing varying barrier heights and quartic potential barriers on each binary junction. This is constructed in the following manner. First we define a new coordinate system on the triangular simplex defined by ϕ_i, $i = 1, 2, 3$

$$(u, v) \mapsto [\phi_1 = uv, \quad \phi_2 = u(1-v), \phi_3 = 1-u]. \tag{57}$$

This consists of lines parallel to constant ϕ_3 (u = constant, $0 < v < 1$) and radial lines from $\phi_3 = 1$ (v = constant, $0 < u < 1$) to the opposite side. We then construct a function

$$f_{DW}(u, v) = 16u^4(1-u/2)^4v^2(1-v)^2, \tag{58}$$

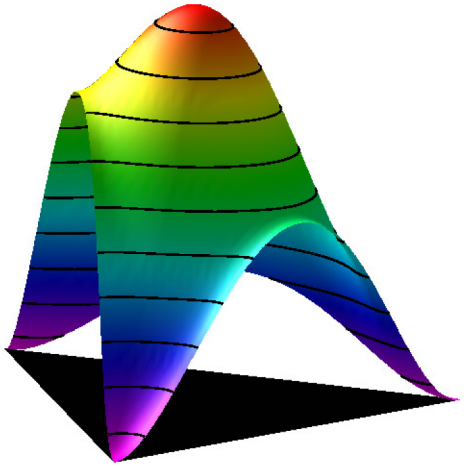

Fig. 1. A generalisation of the Folch potential (for 3 phases) over a triangular simplex with bulk phases located at the three vertices. This construction retains zero derivative normal to the boundary, and has a high point at the triple junction, like the Folch potential. It also has variable barrier heights on the binary junctions (in a ratio, here, of 1:2:3. Such a potential provides gradient driving forces that never leave the simplex.

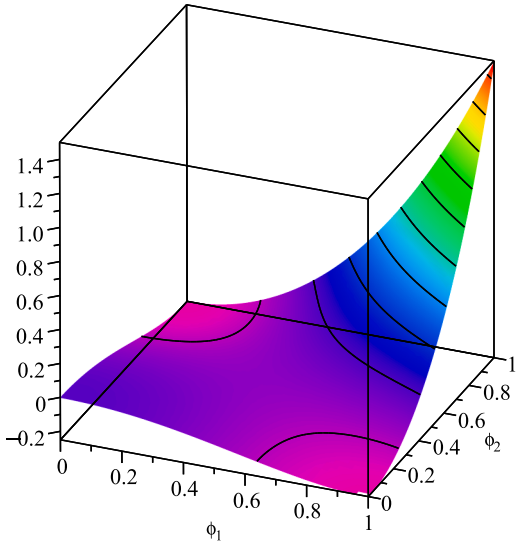

Fig. 2. Shows the potential for multiphase field models without a constraint. The potential is instead modified so that bulk phases are energetically preferred.

which has the property of being zero on two sides of the triangular simplex and quartic on the remaining side, and also zero derivative in the u direction by design on the non-zero edge. We chose the interpolating function (a monotonic function that maps $[0, 1]$ to itself), $16u^4(1-u/2)^4$, over other candidates because it leads to a final polynomial expression (Eq. (60)), which another interpolation may not, e.g. $3u^2-2u^3$ (see later for the effect of using this function).

When transforming back to ϕ_i coordinates using

$$u{=}\phi_1+\phi_2, v=\frac{\phi_1}{\phi_1+\phi_2} \tag{59}$$

we obtain the polynomial function

$$f_{12}=\phi_1^2\phi_2^2(2-\phi_1-\phi_2)^4, \tag{60}$$

and cyclically for the other indices. Note that when $\phi_j+\phi_j=1$, Eq. (60) reduces to $f_{ij}=\phi_i^2\phi_j^2$. We finally set the double well potential of all three contributions using:

$$f_{DW}=\sum_{i<j} W_{ij}f_{ij}. \tag{61}$$

Other multiphase models that do not impose the constrain $\sum_i \phi_i=1$, include [31–35]. Central to this model design is a double well potential typically of the form

$$f_{DW}=\sum_i -\frac{a_1}{2}\phi_i^2+\frac{a_2}{4}\phi_i^4+\frac{a_3}{2}\sum_{i<j}\phi_i^2\phi_j^2 \tag{62}$$

where a_1, a_2, a_3 are chosen so that there is a set of minima in each bulk phase, e.g. $\phi_i=1$, e.g. $a_1=a_2=1$, $a_3=2$. An example of this is shown in Fig. 2 for just two phase fields. There are minima at $\phi_1=1$, $\phi_2=0$ and $\phi_1=0$, $\phi_2=1$. The multiphase field equations take the form

$$\dot{\phi}_i=-M\frac{\delta F}{\delta\phi_i} \tag{63}$$

where by implication the mobility matrix is diagonal: $\mathbf{M}=M\mathbf{I}$. Hence, the constraint is not imposed and indeed is not necessarily met in these models, instead the model construction seeks to make it energetically favourable to be in any one bulk phase.

4.3. Gradient Energy

We have narrowed the choice of double well potential by seeking a construction that is simple, yet still incorporates double index quantities naturally. However, we have not addressed the choice of gradient terms. It is not so easy to assess the gradient terms because of the difficulty of visualising functions of both ϕ_i and $\nabla\phi_i$.

The relations between ϵ^2, W and δ given in Wheeler [4] is

$$\epsilon^2=6\sigma\delta,\quad W=\frac{12\sigma}{\delta} \tag{64}$$

which we wish to reproduce by having a fresh look at the 1D solution. The tanh function has the identity

$$\tanh(x)\equiv\frac{e^x-e^{-x}}{e^x+e^{-x}} \tag{65}$$

and consequently

$$\frac{1}{2}(1+\tanh x/2)=\frac{e^{x/2}}{e^{x/2}+e^{-x/2}}=\frac{1}{1+e^{-x}}. \tag{66}$$

So let us define a flat surface, normal to the x direction. by defining

$$\phi=\frac{1}{1+\exp(x/\delta)}. \tag{67}$$

The interface, when $\phi=\frac{1}{2}$, is thus located at $x=0$. Then

$$\phi'(x)=-\frac{\phi^2}{\delta}\exp(x/\delta)=-\frac{1}{\delta}\phi(1-\phi) \tag{68}$$

and so

$$\frac{1}{2}(\phi')^2=\frac{1}{2\delta^2}\phi^2(1-\phi)^2. \tag{69}$$

Further differentiation of Eq. (68) gives

$$\phi''{=}\frac{-1}{\delta}(1-2\phi)\phi'=\frac{1}{\delta^2}(1-2\phi)(1-\phi)\phi \tag{70}$$

or

$$\phi''=\frac{1}{2\delta^2}\frac{\partial}{\partial\phi}[\phi^2(1-\phi)^2] \tag{71}$$

Noting that the equilibrium equation for the energy functional

$$E=\int\frac{1}{2}\delta^2|\nabla\phi|^2+\frac{1}{2}\phi^2(1-\phi)^2, \tag{72}$$

is

$$\frac{\delta E}{\delta\phi}=-\delta^2\nabla^2\phi+\frac{1}{2}\frac{\partial}{\partial\phi}[\phi^2(1-\phi)^2]=0 \tag{73}$$

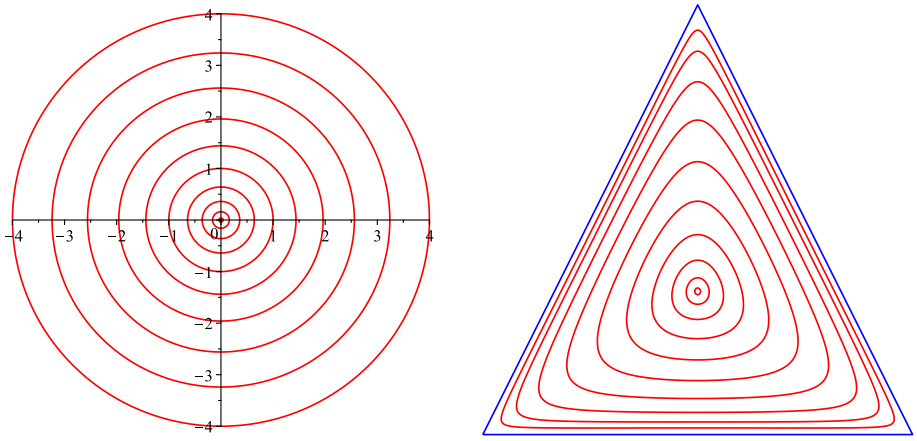

Fig. 3. Mapping of a series of circles on the x, y plane (left) to the triangular simplex (right), using Eq. (83). The origin of the x, y plane maps to the centre of the simplex. Points on the simplex boundary are mapped from infinity in the x, y plane. Such a mapping is a 2D generalisation of the mapping $R \to [-1, 1]: x \mapsto \tanh x$.

we see that ϕ satisfying Eq. (70) also satisfies Eq. (73) and thus the latter has a solution Eq. (67).

Introducing dimensional energy parameters, ϵ and W, we can relate physical surface energy, σ, to these parameters using our 1D equilibrium solution:

$$\sigma = \int_{-\infty}^{\infty} \frac{1}{2}\epsilon^2|\phi_x|^2 + \frac{1}{2}W\phi^2(1-\phi)^2 \mathrm{d}x = \int_{-\infty}^{\infty}\left(\frac{\epsilon^2}{2\delta^2} + \frac{W}{2}\right)\phi^2(1-\phi)^2 \mathrm{d}x$$
$$= \int_0^1 \left(\frac{\epsilon^2}{2\delta} + \frac{W\delta}{2}\right)\phi(1-\phi)\mathrm{d}\phi = \frac{1}{6}\left(\frac{\epsilon^2}{2\delta} + \frac{W\delta}{2}\right), \tag{74}$$

where we use the notation $\phi_x \equiv \phi'(x)$. The most natural way to satisfy this is to set

$$\epsilon^2 = 6\sigma\delta, \quad W = \frac{6\sigma}{\delta} \tag{75}$$

where we find that we do not reproduce Wheeler's result, [4], Eq. (64), and so use Eq. (75) from hereon.

Using this, multiphase generalises as

$$\epsilon_{ij}^2 = 6\sigma_{ij}\delta_{ij}, \tag{76}$$

$$W_{ij} = \frac{6\sigma_{ij}}{\delta_{ij}} \tag{77}$$

A constant interface width model has $\delta_{ij} = \delta$ so that

$$\epsilon_{ij}^2 = 6\sigma_{ij}\delta \tag{78}$$

$$W_{ij} = \frac{6\sigma_{ij}}{\delta}. \tag{79}$$

On the other hand, a model that we advocate in Section 6 is where surface energy is proportional to interface width,

$$\sigma_{ij} = W\delta_{ij}/6, \tag{80}$$

where W is a constant with units of energy density. This gives

$$\epsilon_{ij}^2 = W\delta_{ij}^2 \tag{81}$$

$$W_{ij} = W, \tag{82}$$

all constant and equal.

We cannot, and do not, state that physical interface widths, δ_{ij} are proportional to their respective binary surface energies. We do find, though, in Section 6, that making this assumption allows us to control triple angles in a relatively natural manner. This is by establishing a formulation for equal triple junction angles and then transforming the formulation to arbitrary angles. This not only changes the angles at the junction, but also changes the interface widths, δ_{ij}.

5. A multiphase solution

Having considered the manipulation of a 1D solution to produce a single phase model. We now construct an analogous 2D solution for three multiphase fields, ϕ_i. Our motivation is to use these phase fields to illustrate and analyse the gradient function term in the free energy. For this mapping, $\phi_1(x, y)$, $\phi_2(x, y)$ and $\phi_3(x, y)$, we can, for example, evaluate gradient fields such as $q(x, y) = \sum_i \nabla\phi_i \cdot \nabla\phi_i$. If, further, the mapping is one-one and invertible, we can associate q for every value of ϕ_i, $i = 1..3$ in the simplex. This allows us to see the relation $\tilde{q}(\bar{\phi}) \equiv q(\mathbf{x}(\bar{\phi}))$, i.e. q as a function of ϕ_1, ϕ_2 and ϕ_3.

We now postulate a 2D multiphase solution, which is a generalisation of the tanh profile. Our only guide being: to use something analogous to the 1D case for each field; the solution has a triple junction; behaves like a two phase field away from the triple junction; and that the sum of these fields must be unity. Define three equal length normals to three interfaces such that their sum, $\mathbf{n}_{12} + \mathbf{n}_{23} + \mathbf{n}_{31} = \mathbf{0}$ (an equilateral triangle, but we relax the equal length constraint later). Using $x_{ij} \equiv \mathbf{x}\cdot\mathbf{n}_{ij}$, which implies $x_{12} + x_{23} + x_{31} = 0$ and $x_{ij} = -x_{ji}$,we postulate a set of phase fields:

$$\phi_1 = \frac{1}{1 + e^{x_{12}} + e^{x_{13}}} \tag{83}$$

and cyclically for the other phase fields, ϕ_2, ϕ_3. These fields fortunately have the property

$$\phi_1 + \phi_2 + \phi_3 = 1 \tag{84}$$

without further manipulation.

A visualisation of the mapping Eq. (83) (and cyclically) is shown in Fig. 3. On the left the axes are the cartesian x, y and on the right the 3 simplex so that any value of $\bar{\phi}$ is located within. Any point $\mathbf{x}_0 = (x_0, y_0)$ maps to a unique point $\bar{\phi}_0$ in the 3 simplex on the right, and the circles on the left map to closed curves on the right. The diagram reveals that the mapping is one-one and invertible, with the origin mapping to the centre of the triangle and infinity mapping to the boundary of the simplex.

To get a better feel for the functions, Eq. (83), consider the limiting case where $\mathbf{x}\cdot\mathbf{n}_{12}$ is near zero, and $\mathbf{x}\cdot\mathbf{n}_{13} \to -\infty$, then

$$\phi_1 \approx \frac{1}{1 + e^{x_{12}}} \tag{85}$$

as in Eq. (66). Thus binary junctions are found, in (x, y) space, well away from the origin in a direction normal to any of the sides of the triangle defined by the three normals.

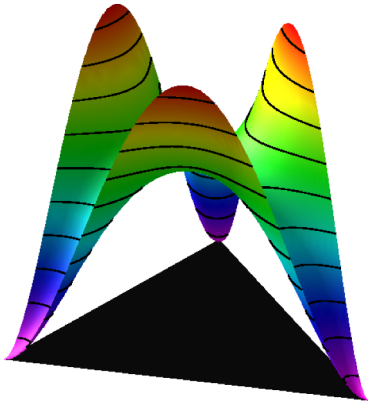

Fig. 4. Tiaden-Nestler-Wheeler gradient energy, Eq, (46), has a severe low value at the triple junction. The black triangle at the base represents the 3 simplex ϕ_1, ϕ_2, ϕ_3 such that $\sum_i \phi_i = 1$.

5.1. Visualising and constructing the gradient term

Using the multiphase field, Eq. (83), we visualise the gradient term for different models, and also construct a gradient term that matches a potential.

Using the constructed solution we can plot each candidate gradient energy as a function of ϕ_i to inspect their characteristics. We do this in Figs. 4–7, being the gradient terms of the models detailed in Eqs. (46)–(49) and a model to be developed subsequently, respectively. Here we see the energy profile for each model. In particular the model Eq. (46) displays a local minimum at the triple point precisely analogous to the energy profile of the double well potential, $\sum_{i<j} \phi_i^2\phi_j^2$. One observation is that 47 and 48 have identical energy profiles (for constant W_{ij}) as they should since one can add multiples of $|\sum_i^n \nabla\phi_i|^2 = 0$ to any gradient term. We note that these do not have global maximum at the triple junction. The model postulated here for no other reason than simplicity, Eq. (49), has a more attractive energy profile, and finally, a gradient energy model that matches the Folch exactly is shown in Fig. 7. We should emphasise that the equilibrium solution for each choice of gradient term will not match our analytical solution and therefore the actual shape of the gradient energy function as a function of phases, ϕ_i will not be as shown in Figs. 4–7, which we can only take as indicative.

We naturally wish to constrain our free energy constructions so that they reduce correctly on binary junctions, but agreement on the simplex edge is insufficient to guarantee a correct multiphase construction, which we feel must have similar properties to the potential term, e.g. a maximum at the triple junction and zero normal gradients on the boundary of the simplex. To this end we examine again the Folch-Plapp double well potential

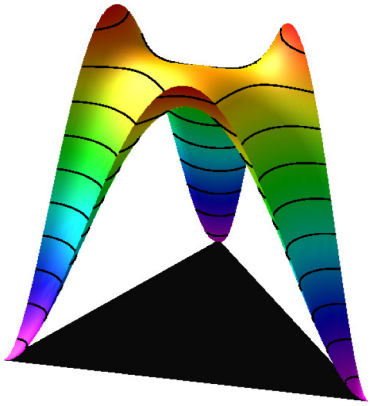

Fig. 5. Folch-Plapp-Toth-Steinbach-Piazola model, Eqs. (47) and (48) has a small local maximum at the triple point), but a pronounced maximum at the binary junction.

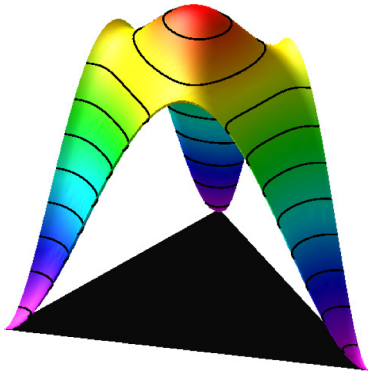

Fig. 6. A proposed gradient energy construction, Eq. (49), has a maximum at the triple junction, but minima near the binary junctions.

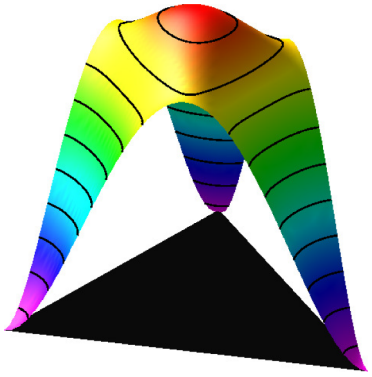

Fig. 7. New proposed gradient energy construction, Eq. (95), has a maximum at the triple junction, correct saddle points at the binary junctions. In fact this is designed to match the Folch-Plapp potential, $\sum_i \phi_i^2(1-\phi_i)^2$.

$$f_{DW} = \sum_{i=1}^{3} \phi_i^2(1-\phi_i)^2/2. \tag{86}$$

This has all the correct properties and has the benefit of being a low order polynomial. Certainly, for say, $\phi_3 = 0$, $\phi_1 = \phi = (1-\phi_2)$,

$$f_{DW} = \phi^2(1-\phi)^2. \tag{87}$$

It is instructive to use our multiphase solution Eq. (83) to plot this potential over x, y space as shown in Fig. 8, where it is worth observing the higher energy over the triple junction.

But it is also useful to inspect its properties along the line defined by $\phi_3 = \phi$, $\phi_1 = \phi_2 = (1-\phi)/2$. This is given by

$$\frac{1}{16}(-1+\phi)^2(9\phi^2+2\phi+1) \tag{88}$$

and shown in Fig. 9. Using this function, and inspecting the relations between phases of Eq. (83) we were able to construct the following gradient function

$$f_G = -\sum_{i<j} \frac{1}{2}(\phi_i+\phi_j)[4-3(\phi_i+\phi_j)]\nabla\phi_i\cdot\nabla\phi_j \tag{89}$$

which equals the Folch-Plapp double well potential, Eq. (86), throughout the simplex (for three phases only). At this point we can postulate an alternative surface energy model to [1] that avoids the functions of $\bar{\phi}$ outside the summation:

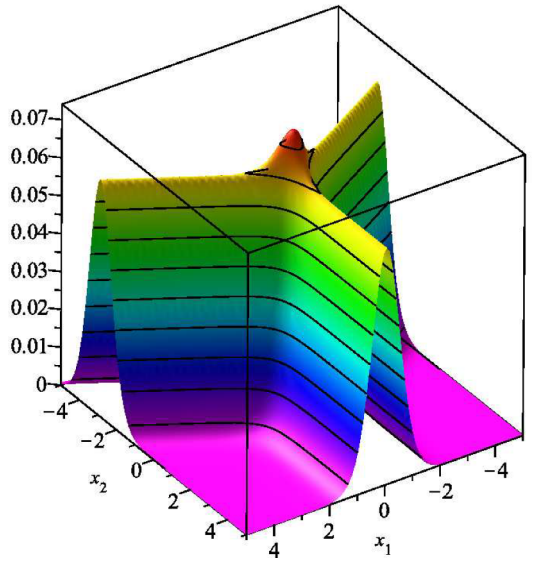

Fig. 8. This is a plot of the Folch-Plapp potential over the multiphase solution Eq. (83).

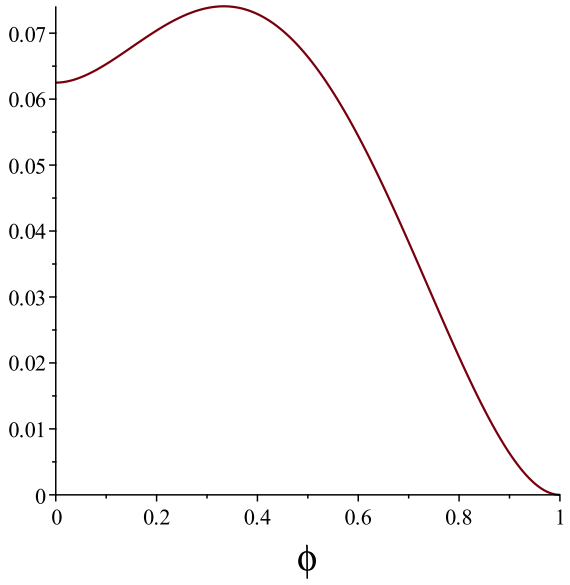

Fig. 9. View of the Folch-Plapp double well potential from the bulk of one phase to the middle of the binary junction of the other two phases. This function has zero gradients at the extremes and a maximum at $\phi = 1/3$.

$$f = -\sum_{i<j}^{3} \tfrac{1}{2}\epsilon_{ij}^2(\phi_i+\phi_j)[4-3(\phi_i+\phi_j)]\nabla\phi_i\cdot\nabla\phi_j + \sum_{i<j}^{3} W_{ij}\phi_i^2\phi_j^2(2-\phi_i-\phi_j)^4 \tag{90}$$

At this stage, we only state this formulation as being a plausible alternative to that found in [1]. On inspecting the double well potential for higher values of $n = 3$ we find that $n = 4$ gives a higher potential for $\phi_i = 1/4$, $i = 1, 4$, but this feature does not extend to higher values of $n > 4$. This issue is rectified by choosing a lower order interpolating function for $f(u, v)$ in Eq. (58), i.e.

$$f_{DW}(u,v) = (3u^2-2u^3)v^2(1-v)^2 \tag{91}$$

This gives the double well potential

$$f_{DW} = \sum_{i<j}^{n} W_{ij}\frac{3-2\phi_i-2\phi_j}{(\phi_i+\phi_j)^2}\phi_i^2\phi_j^2 \tag{92}$$

and so the more general formulation is

$$f = -\sum_{i<j}^{n} \tfrac{1}{2}\epsilon_{ij}^2(\phi_i+\phi_j)[4-3(\phi_i+\phi_j)]\nabla\phi_i\cdot\nabla\phi_j + \sum_{i<j}^{n} W_{ij}\tfrac{3-2\phi_i-2\phi_j}{(\phi_i+\phi_j)^2}\phi_i^2\phi_j^2 \tag{93}$$

where, for constant interface width, we have

$$f = -\sum_{i<j}^{n} W_{ij}\{\tfrac{1}{2}\delta_0^2(\phi_i+\phi_j)[4-3(\phi_i+\phi_j)]\nabla\phi_i\cdot\nabla\phi_j + \tfrac{3-2\phi_i-2\phi_j}{(\phi_i+\phi_j)^2}\phi_i^2\phi_j^2\} \tag{94}$$

Despite this model reducing correctly across each binary junction, we find, computationally, that it does not reproduce the theoretical angles at the triple junction. That said we postulate that such a model may well benefit from the addition of a hump potential such as advocated in [1] (see Appendix B for an indication of the properties of such a function).

We now focus the paper on a more rigorously derived formulation that necessarily produces the correct triple junction angles. We seek to generalise the Folch-Plapp formulation, [2], which we write in the form

$$F_S = \int \delta^2 \sum_{i}^{3} \nabla\phi_i\cdot\nabla\phi_i + \phi_i^2(1-\phi_i)^2. \tag{95}$$

which has a 1D equilibrium solution with only two phases present:

$$\phi_1 = 1-\phi_2 = \frac{1}{1+\exp(x/\delta)}, \phi_3 = 0. \tag{96}$$

6. Energy formulation to control triple junction angle

We seek a generalisation with a stronger mathematical underpinning: one that mathematically guarantees that the theoretically correct triple junction angles are recovered. Before doing this we wish to illustrate a key transformation in a simpler 1D setting. Consider two 1D solutions, ϕ^0 and ϕ, that differ only in their interface width:

$$\phi^0 = \frac{1}{1+\exp(x)} \tag{97}$$

and

$$\phi = \frac{1}{1+\exp(x/\delta)}. \tag{98}$$

By writing $X = x/\delta$ so that

$$\phi = \frac{1}{1+\exp(X)}, \tag{99}$$

we find by the chain rule that

$$\mathrm{d}\phi_0 = \frac{\partial\phi_0}{\partial \mathrm{x}}\frac{\partial \mathrm{x}}{\partial \mathrm{X}}\frac{\partial \mathrm{X}}{\partial\phi}\mathrm{d}\phi. \tag{100}$$

At a point $x = X = 0$

$$\left.\frac{\partial\phi_0}{\partial x}\right|_0 = 1/\left.\frac{\partial X}{\partial\phi}\right|_0 \tag{101}$$

and so at $x = X = 0$

$$\mathrm{d}\phi_0 = \frac{\partial \mathrm{x}}{\partial \mathrm{X}}\mathrm{d}\phi = \delta\mathrm{d}\phi. \tag{102}$$

Following the above as a template for multiphase, we use the solution Eq. (83) as a reference solution, and introduce the notation ϕ_i^0 to distinguish it from the general solution, ϕ_i. Thus, in a slightly different

from Eq. (83):

$$\frac{1}{\phi_1^0} = 1 + \exp(x_{12}) + \exp(x_{13}), \frac{1}{\phi_2^0} = 1 + \exp(x_{23}) + \exp(x_{21}), \frac{1}{\phi_3^0} = 1 + \exp(x_{31}) + \exp(x_{32}) \tag{103}$$

and consider that this is defined in a plane that passes through the 3D points $\mathbf{e}_1 \equiv [1, 0, 0]$, $\mathbf{e}_2 \equiv [0, 1, 0]$, $\mathbf{e}_3 \equiv [0, 0, 1]$, with normals, $\mathbf{n}_{ij} = \mathbf{e}_j - \mathbf{e}_i$. In this coordinate system we can write this as

$$\frac{1}{\phi_1^0} = 1 + \exp(x - y) + \exp(x - z), \frac{1}{\phi_2^0} = 1 + \exp(y - z) + \exp(y - x), \frac{1}{\phi_3^0} = 1 + \exp(z - x) + \exp(z - y) \tag{104}$$

which can be written in terms of just two coupled variables on the right-hand side, $(x - y)$ and $(y - z)$,

$$\frac{1}{\phi_1^0} = 1 + \exp(x - y) + \exp(x - y)\exp(y - z), \frac{1}{\phi_2^0} = 1 + \exp(y - z) + 1/\exp(x - y) \tag{105}$$

and so we find that

$$\exp(x_{12}) \equiv \exp(x - y) = \frac{\phi_2^0}{\phi_1^0} \tag{106}$$

and in general

$$\mathbf{x}\cdot\mathbf{n}_{ij} \equiv x_{ij} = \ln(\phi_j^0) - \ln(\phi_i^0). \tag{107}$$

By using the substitution $\phi_3^0 = 1 - \phi_1^0 - \phi_2^0$ and fixing a plane through $(x + y + z = 0)$, we find the inverse transformation Eq. (104):

$$\begin{pmatrix} x \\ y \\ z \end{pmatrix} = \begin{pmatrix} -2/3 & 1/3 & 1/3 \\ 1/3 & -2/3 & 1/3 \\ 1/3 & 1/3 & -2/3 \end{pmatrix} \begin{pmatrix} \ln(\phi_1^0) \\ \ln(\phi_2^0) \\ \ln(\phi_3^0) \end{pmatrix}. \tag{108}$$

Eq. (104) and its inverse, Eq. (108) relate to an equal angle triple junction. We now consider, the more arbitrary solution where all three angles can vary by tilting the equal angle solution as follows:

$$\frac{1}{\phi_1} = 1 + \exp(x/\delta_1 - y/\delta_2) + \exp(x/\delta_1 - z/\delta_3) \tag{109}$$

and cyclically. By writing Eq. (109) in the equivalent form

$$\frac{1}{\phi_1} = 1 + \exp(X - Y) + \exp(X - Z) \tag{110}$$

where $X = x/\delta_1$ etc, we have

$$\begin{pmatrix} X \\ Y \\ Z \end{pmatrix} = \begin{pmatrix} -2/3 & 1/3 & 1/3 \\ 1/3 & -2/3 & 1/3 \\ 1/3 & 1/3 & -2/3 \end{pmatrix} \begin{pmatrix} \ln(\phi_1) \\ \ln(\phi_2) \\ \ln(\phi_3) \end{pmatrix}. \tag{111}$$

Using this we find that

$$X - Y \equiv X_{ij} \equiv \mathbf{x}\cdot\mathbf{N}_{ij} = \ln(\phi_j) - \ln(\phi_i) \tag{112}$$

where $\mathbf{N}_{ij}$ represents a triple junction where angles are not necessarily equal. If we define the reference function

$$\phi_i^0 = \hat{\phi}_i(x, y, z), \tag{113}$$

then the general multiphase field is given, *using the same function*, by

$$\phi_i = \hat{\phi}_i(X, Y, Z) \tag{114}$$

where $X_i = x_i/\delta_i$. That is, they can be represented by the same function but on a different space. Using this examine

$$\frac{\partial\phi_i^0}{\partial x^a} = \frac{\partial\phi_i^0}{\partial\phi_j}\frac{\partial\phi_j}{\partial x^a} = \left(\frac{\partial\phi_i^0}{\partial x^b}\frac{\partial x^b}{\partial X^A}\frac{\partial X^A}{\partial\phi_j}\right)\frac{\partial\phi_j}{\partial x^a}. \tag{115}$$

Now the term in the bracket can be written

$$R_{ij} \equiv \frac{\partial\phi_i^0}{\partial\phi_j} = \frac{\partial\phi_i^0}{\partial x^b}\frac{\partial x^b}{\partial X^A}\frac{\partial X^A}{\partial\phi_j} \equiv J_{ib}D_{bA}(J^{-1})_{Aj}. \tag{116}$$

Since the left hand side and right hand side of the final term are inverse matrices of each other and the middle matrix $\mathbf{D}$ is a diagonal matrix

$$\mathbf{D} \equiv \begin{pmatrix} \delta_1 & 0 & 0 \\ 0 & \delta_2 & 0 \\ 0 & 0 & \delta_3. \end{pmatrix}. \tag{117}$$

From Eq. (104) we have

$$-\frac{\mathrm{d}\phi_1^0}{\phi_1^2} = \exp(x - y)(\mathrm{dx} - \mathrm{dy}) + \exp(\mathrm{x} - \mathrm{z})(\mathrm{dx} - \mathrm{dz}) \tag{118}$$

At the midpoint, $\phi_i = 1/3$, $x = y = z = 0$ we have

$$\begin{pmatrix} \mathrm{d}\phi_1^0 \\ \mathrm{d}\phi_2^0 \\ \mathrm{d}\phi_3^0 \end{pmatrix} = \frac{1}{9}\begin{pmatrix} -2 & 1 & 1 \\ 1 & -2 & 1 \\ 1 & 1 & -2 \end{pmatrix}\begin{pmatrix} \mathrm{dx} \\ \mathrm{dy} \\ \mathrm{dz} \end{pmatrix} \tag{119}$$

If we further use the knowledge that $\mathrm{dx} + \mathrm{dy} + \mathrm{dz} = 0$ we find that

$$\mathrm{d}\phi_{\mathrm{i}}^0 = -\frac{1}{3}\mathrm{dx_i} \tag{120}$$

and so the inverse relation

$$\mathrm{dX_i} = -3\mathrm{d}\phi_{\mathrm{i}} \tag{121}$$

Consequently from Eq. (116) we have, at the origin:

$$\mathbf{R} = \mathbf{D}. \tag{122}$$

This means that

$$\nabla\phi_i^0\cdot\nabla\phi_j^0 \equiv \nabla\boldsymbol{\phi}^{0T}\nabla\boldsymbol{\phi}^0 = \nabla\boldsymbol{\phi}^T\mathbf{D}\mathbf{D}^{\mathbf{T}}\nabla\boldsymbol{\phi} \tag{123}$$

Thus we postulate the surface energy as being

$$\boxed{f_S = \frac{W}{4}\sum_i [\delta_i^2\nabla\phi_i\cdot\nabla\phi_i + \phi_i^2(1 - \phi_i)^2]} \tag{124}$$

where W can be taken from any of the barrier heights, e.g.

$$W = \frac{6\sigma_{12}}{\delta_{12}} \tag{125}$$

and

$$\delta_{ij} = \frac{6\sigma_{ij}}{W} \tag{126}$$

Finally, we need to relate the single index, δ_i to the double indexed, δ_{ij}. This is readily done since by definition

$$\delta_{ij}^2 = \delta_i^2 + \delta_j^2 \tag{127}$$

which gives on inversion

$$\delta_i^2 = \frac{1}{2}(\delta_{ij}^2 + \delta_{ik}^2 - \delta_{jk}^2), \quad i \neq j \neq k. \tag{128}$$

We need the above relation because the binary surface energies, σ_{ij} relate directly to the binary interface widths by Eq. (80). Eq. (128) appears to present us with a problem in that it is possible that $\delta_i^2 \leqslant 0$. The critical angle, when this occurs is when one of the angles at the triple junction is $\pi/2$. However, computational results demonstrate that this is not a problem, where we find, for example, that even $\delta_1^2 = -1/3$, $\delta_2^2 = \delta_3^2 = 1$, can be simulated successfully.

6.1. Some failed models

It may be useful to the reader to note that we found other variants of the above model to have only limited applicability in simulation. We

find that a formulation of the form

$$f_S = \sum_{i=1}^{3} \delta_i^2 U_i \nabla\phi_i \cdot \nabla\phi_j + \sum_i \phi_i^2(1-\phi_i)^2, \tag{129}$$

where $U_i = \phi_i + 3\phi_j\phi_k$, or $U_i = \phi_i$ develops an instability as the triple junction angle approaches $\pi/2$ (from larger angles). Since there are reports on smaller angles than $\pi/2$ such as the groove angle at solid-solid-liquid triple junction [36,37], there remains a limitation with this model.

We also add, in passing, that the model

$$f_S = \sum_{i<j} -\delta_{ij}^2 \nabla\phi_i \cdot \nabla\phi_j + \sum_i \phi_i^2(1-\phi_i)^2, \tag{130}$$

was stable in simulation but fails to deliver the correct angle at the triple junction despite affecting the interface width in a similar manner to that of Eq. (124) (although this model might be rescued by the addition of a triple junction barrier as in [1]).

6.2. Generalisation to $n > 3$

A more general $n > 3$ has not been explored in this paper, but clearly a good starting point is the model

$$f_S = \sum_{i=1}^{n} \delta_i^2 \nabla\phi_i \cdot \nabla\phi_i + \phi_i^2(1-\phi_i)^2 \tag{131}$$

where the binary interface energies are (still) related by

$$\delta_{ij}^2 = \delta_i^2 + \delta_j^2. \tag{132}$$

For $n = 4$, for example, the distances from the origin in 4D, δ_1, δ_2, δ_3, δ_4, define the vertices of a tetrahedron and so we determine one of the sides by (using the definition Eq. (128)):

$$\begin{aligned}\delta_1^2 &= \frac{1}{2}(-\delta_{23}^2 + \delta_{31}^2 + \delta_{12}^2), \delta_2^2 = \frac{1}{2}(-\delta_{31}^2 + \delta_{12}^2 + \delta_{23}^2), \delta_3^2 \\ &= \frac{1}{2}(-\delta_{12}^2 + \delta_{23}^2 + \delta_{31}^2).\end{aligned} \tag{133}$$

and then again using Eq. (128),

$$\delta_{14}^2 = \delta_1^2 + \delta_4^2, \tag{134}$$

we determine the remaining single index coefficient

$$\delta_4^2 = \delta_{14}^2 - \delta_1^2 = \delta_{14}^2 - \frac{1}{2}(-\delta_{23}^2 + \delta_{31}^2 + \delta_{12}^2). \tag{135}$$

We speculate that only n binary interface energies are independent for $n > 2$.

6.3. Summary

An overview of what we have done:

1. By recognising that a more general solution with arbitrary angles at the triple junction can be produced by an invertible mapping, we rewrite the equal angle formulation, which is specified in terms of the equal angle solution ϕ_i^0, in terms of the general angle solution ϕ_i. This results in a general multiphase model which controls angles at triple junctions via the binary surface energies, σ_{ij}.
2. The mapping makes convenient use of a two dimensional surface in 3D, which gives a more direct relation between the three phases, ϕ_i^0 and the three Cartesian coordinates, x, y, z (than into the 2D coordinates x, y). Moreover, the generalisation to a plane which cuts the coordinate axes at arbitrary points, governed by the interface widths, follows comfortably.
3. The formulation appear computationally stable for all angles at the triple junction apart from the extremes, 0° and 180°.

We finish off with a restatement of the proposed model for the surface energy density

$$\boxed{\begin{gathered} f_S = \tfrac{W}{4} \sum_i [\delta_i^2 \nabla\phi_i \cdot \nabla\phi_i + \phi_i^2(1-\phi_i)^2] \\ W = \frac{6\sigma_{12}}{\delta_{12}} \\ \delta_{ij} = \frac{6\sigma_{ij}}{W} \\ \delta_i^2 = \sum_{j\neq i} \delta_{ij}^2 - \delta_{jk}^2|_{i\neq j\neq k} \end{gathered}} \tag{136}$$

7. Tests and results

7.1. Angle dependent energy minimum

We test directly the model Eq. (136) at a constructed triple junction. We prescribe a triple junction field at the origin in 2D by

$$\begin{aligned}\phi_1 &= \frac{1}{1+\exp x_{12}+\exp x_{13}}, \phi_2 = \frac{1}{1+\exp x_{23}+\exp x_{21}}, \phi_3 \\ &= \frac{1}{1+\exp x_{31}+\exp x_{32}},\end{aligned} \tag{137}$$

where $x_{ij} = \mathbf{x}\cdot\mathbf{n}_{ij}$ and $\mathbf{n}_{12} + \mathbf{n}_{23} + \mathbf{n}_{31} = \mathbf{0}$. By setting $W = 1$, and prescribing δ_i^2 for each phase we can evaluate f_S in Eq. (136) at any point. Furthermore, we can integrate f_S over any domain, D,

$$F_S = \int_D f_S \,\mathrm{d}x\mathrm{d}y \tag{138}$$

to give us the total energy associated with these fields for any chosen set of normals, $\mathbf{n}_{ij}$ (see Fig. 10). By choosing the domain, D to be a large enough circular disc about the origin, and varying one or more of the normals the total energy over D depends on the normals, and thus the angles at the triple junction. What we seek in doing this is the set of angles that gives an energy minimum. This then can be compared with the theoretical set of angles associated with the choice of δ_i^2. We limit this test to that in which two angles are equal so that the energies will be a function of the remaining angle, θ, only, i.e. $F_S(\theta)$.

In Fig. 11 the sub Fig. 11a–f each give a range of $F_S(\theta)$ for a different choice $\delta_1 = \delta_2 = 1$ and $\delta_3 = 0.7, 0.8, 0.9, 1.0, 2.0, 4.0$, which correspond to the theoretical angles: 109°, 113°, 117°, 120°, 143° and 160° respectively. For example, $\delta_1 = 1$, $\delta_2 = 1$, $\delta_3 = 2$ corresponds to a triangle with vertices, in 3D, [1, 0, 0], [0, 1, 0], [0, 0, 2], with length sides $\sqrt{2}$, $\sqrt{5}$, $\sqrt{5}$, with smallest angle $2\sin^{-1}(1/\sqrt{10}) = 37$ degrees and therefore the largest angle in the triple junction being $180 - 37 = 143$ degrees (used in Fig. 11e). For a wide range of cases the theoretical angle is well approximated by the minimum of $F_S(\theta)$.

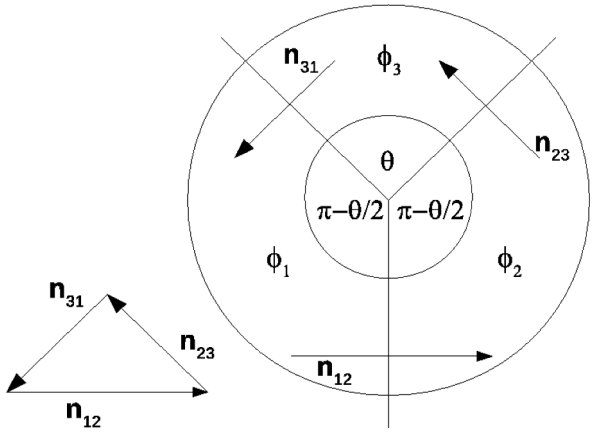

Fig. 10. Circular disc containing three phases, ϕ_1, ϕ_2 and ϕ_3, at the triple junction. The angle, θ is made to vary by keeping $|\mathbf{n}_{31}| = |\mathbf{n}_{23}|$ fixed and varying $\mathbf{n}_{12}$. By integrating over the disc we obtain an energy, $F_S(\theta)$ as a function of θ.

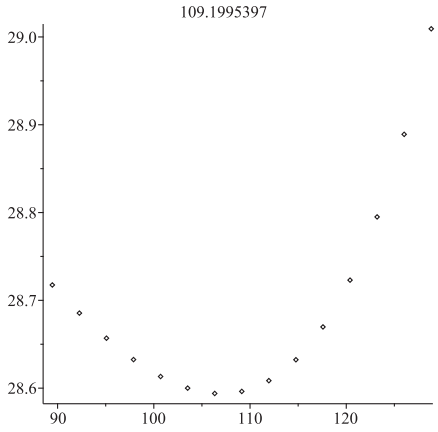

(a) Theoretical angle 109°; computed angle $106 \pm 1°$; $\delta_3 = \delta_2 = 1, \delta_1 = 0.7$

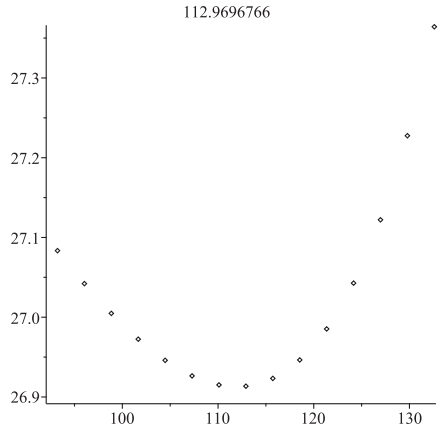

(b) Theoretical angle 113°; computed angle $113 \pm 1°$; $\delta_3 = \delta_2 = 1, \delta_1 = 0.8$

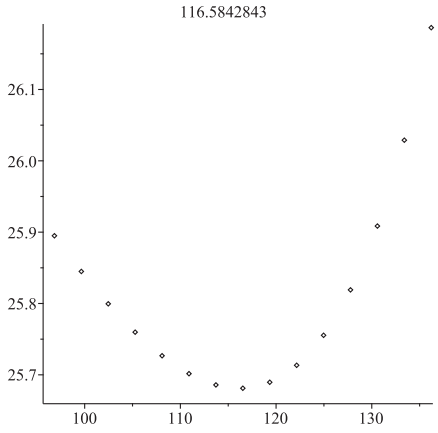

(c) Theoretical angle 117°; computed angle $117 \pm 1°$; $\delta_3 = \delta_2 = 1, \delta_1 = 0.9$

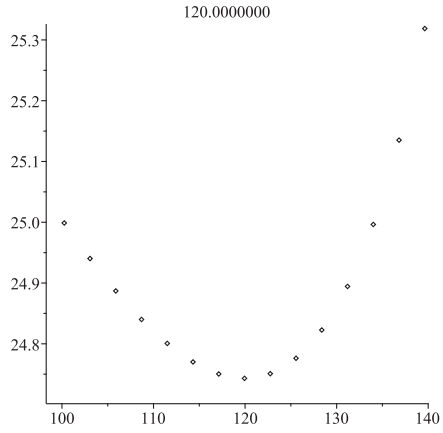

(d) Theoretical angle 120°; computed angle $120 \pm 1°$; $\delta_3 = \delta_2 = 1, \delta_1 = 1.0$

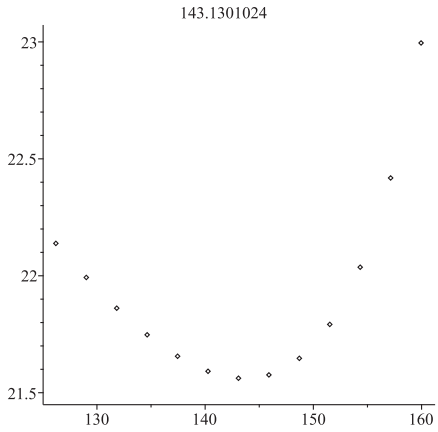

(e) Theoretical angle 143°; computed angle $143 \pm 1°$; $\delta_3 = \delta_2 = 1, \delta_1 = 2.0$

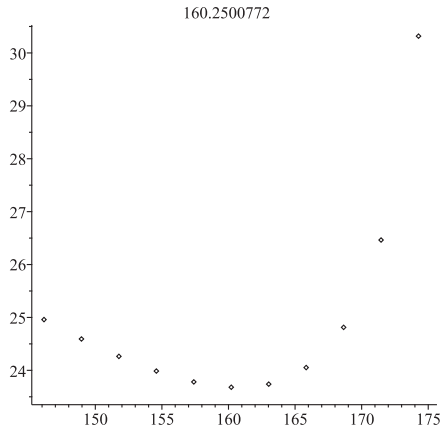

(f) Theoretical angle 160°; computed angle $160 \pm 1°$; $\delta_3 = \delta_2 = 1, \delta_1 = 4.0$

Fig. 11. (a)–(f) Show the energy as the angle sweeps around the theoretical angle.

Clearly, almost any formulation that treats all phases equally will return an optimum angle as $\theta = 2\pi/3 = 120°$. However, one formulation [28] actually had a maximum energy at this angle. We have only given our model's results for these sweeps as none of the other models came close when the angle varied from 120°.

7.2. Phase field implementation

We now examine how our postulated model behaves in phase field under dynamic conditions close to equilibrium, where we expect there to be some flattening or sharpening of the eutectic interface curves due

Table 2
Table of values for the phase field simulation.

Parameter	Value
M	0.01
$\delta_3 = \delta_2$	0.4
δ_1	Multiples of δ_3
ΔT	0.05
Domain size	32×16
Mesh size	$\Delta x = 0.125$
Length unit	1 nm
Time unit	0.67 ns
Initial eutectic length	3 (x-direction)
Initial lamellae width	2×16 (y-direction)
Common tangents:	$c_1 = 1/2$, $c_2 = 1/4$, $c_3 = 3/4$

to our method of implementation of the binary surface energies, σ_{ij}.

The phase field implementation for these tests uses Model Eq. (136) with mobility model given by Eq. (17), and a bulk force to be described. The model used is a simplest example model where each of the three free bulk energies are represented by quadratics and the diffusion throughout the domain is constant. We also adopt the following bulk free energy:

$$f_B = g_1 f_1 + g_2 f_2 + g_3 f_3 \tag{139}$$

where $g_i = g(\phi_i)/\sum g(\phi_i)$ with $g(\phi) = 3\phi^2 - 2\phi^3$, are interpolation functions, and

$$\begin{aligned} f_1 &= [c - c_1 + (c_1 - c_2)g_2 + (c_1 - c_3)g_3]^2 + g_1 \Delta T, f_2 \\ &= [c - c_2 + (c_2 - c_3)g_3 + (c_2 - c_1)g_1]^2 + g_1 \Delta T, f_3 \\ &= [c - c_3 + (c_3 - c_1)g_1 + (c_3 - c_2)g_2]^2 + g_1 \Delta T. \end{aligned} \tag{140}$$

The concentrations c_i are from common tangent construction and are given in Table 2 along with other parameters for the simulation. Note that when $g_1 = 1$, we have $f_1 = (c - c_1)^2 + \Delta T$; when $g_2 = 1$ we have $f_2 = (c - c_2)^2$; and when $g_3 = 1$ we have $f_3 = (c - c_3)^2$. All three of which are the bulk free energies of the pure three phases. Thus the combination in Eq. (139) is a phase dependent interpolation. We adopt this interpolation technique over the WBM method to minimise spurious phase generation between any two phases (see [7,8] for further discussion).

Fig. 12(a)–(d) show solute profile contours from the multiphase field simulation. Superimposed on the plot is the theoretically correct equilibrium angle corresponding the input, δ_i. These results show the effect of differing binary surface energy terms on the manner of growth in this dynamic setting with a clear flattening off of the curved surface

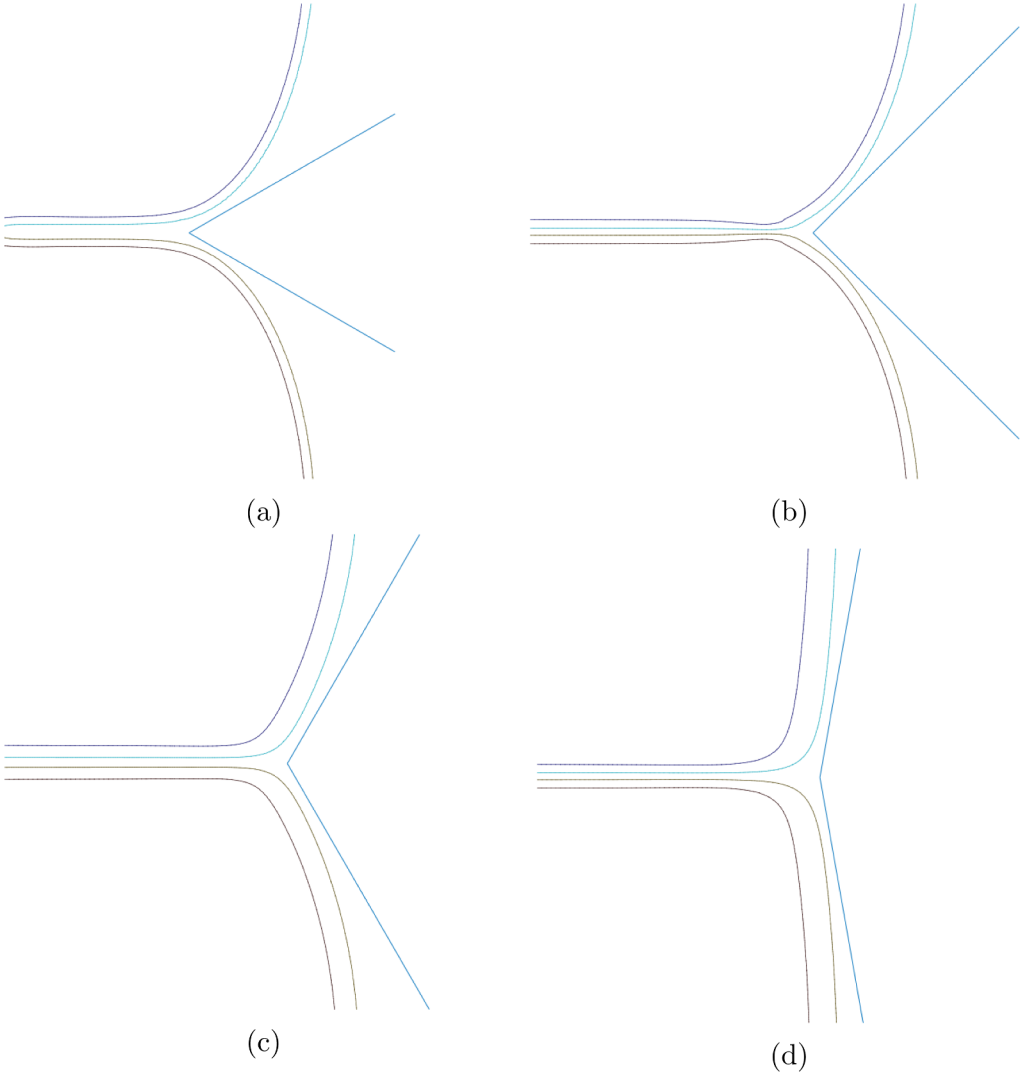

Fig. 12. (a)–(d) Show simulation results using the new model Eq. (124). The contours of the solute profile and the theoretical angles (60°, 90°, 120° and 60°, respectively), are shown superimposed for direct comparison. The values for δ_i^2 are $-1/3$, 0, 1, 16 respectively. A distinctive feature of the model is the relation between angle and interface width, so that, for example,the liquid solid interface increases with angle.

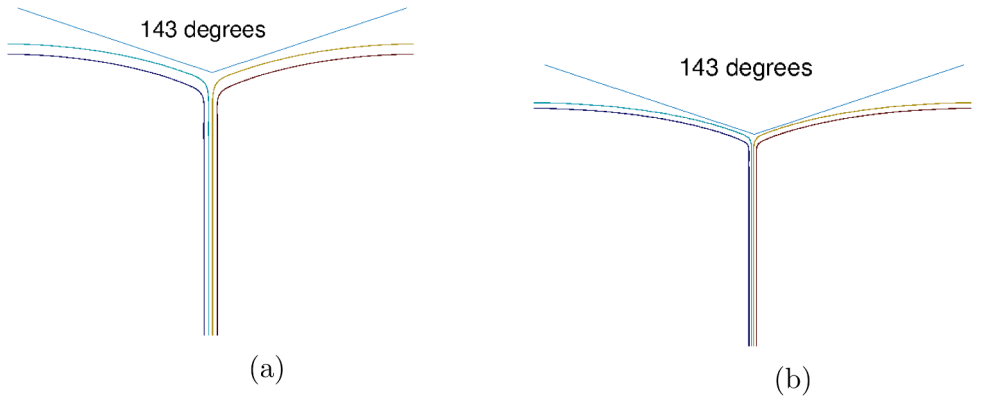

Fig. 13. (a) and (b) show simulation results for 143°, and also with $U_i = \phi_i + 3\phi_j\phi_k$ (rather than $U_i = 1$ as in Eq. (124)) and with increasingly finer interface widths.

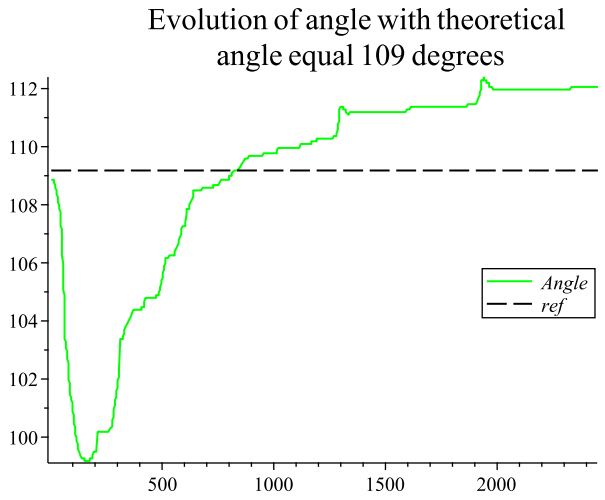

Fig. 14. The evolution of the angle at the triple junction in time in units of 0.67 ns. The initial condition sets the correct angle but the symmetric boundary condition and growth changes the profile.

approaching the tangent indicated by the equilibrium correct angle. These eutectics grow from the left, and though they have evolved towards a steady velocity state they are not in an equilibrium state. We choose a small value of ΔT to give near equilibrium behaviour, but the boundary conditions being symmetric guarantee that the liquid-solid interfaces are curved.

Because of the curvature at the interface it is difficult to prescribe a quantitative measure of angle. One such measure is given by

$$\theta_1 = \cos^{-1}(\mathbf{n}_{12}\cdot\mathbf{n}_{13}) \tag{141}$$

(and cyclically) where

$$\mathbf{n}_{ij} = \frac{\int(\phi_j\nabla\phi_i - \phi_i\nabla\phi_j)H(\bar{\phi})\mathrm{dxdy}}{|\int(\phi_j\nabla\phi_i - \phi_i\nabla\phi_j)H(\bar{\phi})\mathrm{dxdy}|} \tag{142}$$

and $H(\bar{\phi})$ is some function that limits the integration area to the vicinity of the triple junction. If H is too local then the angle will be too small and, conversely, if too large (e.g. $H = 1$) the angle will be too large. Using $H = \phi_1\phi_2\phi_3$ we found we could reproduce the angles between 100 and 143 within a couple of degrees, see for example Fig. 14, but were less successful outside this region. That said the superposition of the correct angle on the eutectic simulation results in Fig. 12 clearly show the model works well even in this dynamic setting. Further narrowing of the interface width has the effect shown in Fig. 13, which suggests that in the limit of near equilibrium and zero interface width the theoretical angle is approached at the triple junction as the interfaces become sharp.

8. Conclusion

Commencing with a review we have narrowed the field of possible multiphase models to a handful. We have developed some new tools that not only narrow the field of candidates, but create new ones.

In seeking a consistent model that allows binary interface energies to be incorporated into the model in a way that correctly reduces to a single phase formulation, we postulated the model Eq. (90). This incorporated a potential well that allows barrier heights proportional to the binary surface energies, which in turn facilitated the future development of a model that keeps interface widths equal. However, unlike the model found in [1], computation with this model does not return correct theoretical angles. This illustrates that correct reduction across any binary junction is not sufficient to reproduce triple junction angles correctly, and so modification by the addition of triple junction terms becomes mandatory.

In Section 6 we postulate a more rigorous theoretically justified multiphase field model for alloy solidification, Eq. (136). This incorporates binary surface energies, σ_{ij}, in a manner that mathematically guarantees the correct reproduction of triple junction angles between phases. In deriving this model we have made use of an analytical multiphase solution, Eq. (104). The analytical solution is modified by changing the underlying arbitrary triangle, which suggests that an affine transformation of an equal angle formulation will deliver the sought after general formulation. The only potential down side of this is that the relative interface widths, δ_{ij} vary with the binary interface energies, σ_{ij}.

Implementing the model Eq. (136) together with a simple bulk energy model we find that the effect of the binary surface on the eutectic growth is largely in line with the angles expected at equilibrium. This observation is further backed up by integrating the energy field as a function of underlying fields with varying angles, and finding that the correct angle implied by the binary surface energies is at a minimum at that angle - see Fig. 11.

CRediT authorship contribution statement

P.C. Bollada: Formal analysis, Conceptualization, Validation, Software, Writing - original draft, Investigation, Methodology, Visualization. **P.K. Jimack:** Writing - review & editing. **A.M. Mullis:** Supervision, Funding acquisition, Writing - review & editing, Project administration.

Declaration of Competing Interest

The authors declare that they have no conflict of interest.

Acknowledgements

This research was funded by EPSRC Innovative Manufacturing Research Hub in Liquid Metal Engineering (LiME), Grant No. EP/N007638/1.

Appendix A. Plotting gradient functions over the simplex

We present this section to give a clear exposition of how to convert scalar gradient functions of phase to functions of phase only using Eq. (104). Beginning with 104, but dropping the superscript ^{0}, we find that

$$-\frac{\mathrm{d}\phi_1}{\phi_1^2}=\exp(x-y)(\mathrm{dx}-\mathrm{dy})+\exp(\mathrm{x}-\mathrm{z})(\mathrm{dx}-\mathrm{dz})=\frac{\phi_2}{\phi_1}(\mathrm{dx}-\mathrm{dy})+\frac{\phi_3}{\phi_1}(\mathrm{dx}-\mathrm{dz}) \tag{A.1}$$

so that

$$-\mathrm{d}\phi_1=\phi_2\phi_1(\mathrm{dx}-\mathrm{dy})+\phi_3\phi_1(\mathrm{dx}-\mathrm{dz}). \tag{A.2}$$

We then make the cartesian identification $\mathrm{dx}=\mathbf{i}$, $\mathrm{dy}=\mathbf{j}$, $\mathrm{dz}=\mathbf{k}$ and $\mathrm{d}\phi_1=\nabla\phi_1$ to write

$$-\nabla\phi_1=\phi_2\phi_1(\mathbf{i}-\mathbf{j})+\phi_3\phi_1(\mathbf{i}-\mathbf{k}). \tag{A.3}$$

and similarly

$$-\nabla\phi_2=\phi_3\phi_2(\mathbf{j}-\mathbf{k})+\phi_1\phi_2(\mathbf{j}-\mathbf{i})-\nabla\phi_3=\phi_1\phi_3(\mathbf{k}-\mathbf{i})+\phi_2\phi_3(\mathbf{k}-\mathbf{j}). \tag{A.4}$$

Hence, for example,

$$\nabla\phi_1\cdot\nabla\phi_1=2\phi_1^2\phi_2^2+2\phi_1^2\phi_2\phi_3+2\phi_1^2\phi_3^2 \tag{A.5}$$

and consequently

$$\frac{1}{2}\sum_{i=1}^{3}\nabla\phi_i\cdot\nabla\phi_i=2\sum_{i<j}\phi_i^2\phi_j^2+\phi_1^2\phi_2\phi_3+\phi_2^2\phi_3\phi_1+\phi_3^2\phi_1\phi_2,=2\sum_{i<j}\phi_i^2\phi_j^2+\phi_1\phi_2\phi_3(\phi_1+\phi_2+\phi_3)=2\sum_{i<j}\phi_i^2\phi_j^2+\phi_1\phi_2\phi_3 \tag{A.6}$$

Appendix B. Gradient energy equivalent of the hump function

Somewhat tangential to the main argument of our paper, but of interest, is an observation regarding a "hump" function, which is similar to that used in [1] to control angles ([1] use its square root). This is given by

$$f_H=(\phi_1\phi_2\phi_3)^2, \tag{B.1}$$

which has the property of being zero and has zero gradient on the simplex boundary. A plot of how this energy varies as a function of one normal varying is given in Fig. B.15 together with an equivalent cross product gradient term (that agrees at 120 degrees)

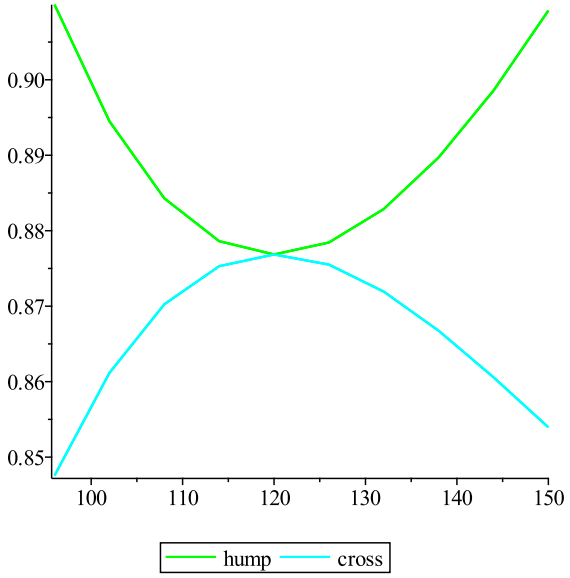

Fig. B.15. Energy as a function of one angle around a triple junction for both the hump function (green) and cross term (cyan). By construction the two energies agree at the 120 deg angle.

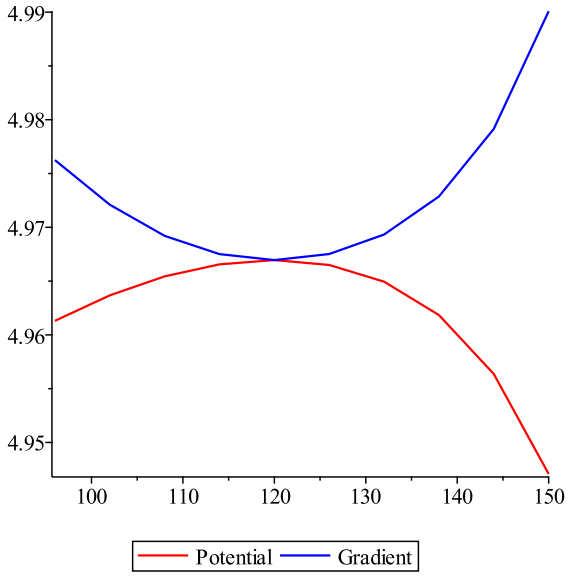

Fig. B.16. Energy as a function of one angle around a triple junction for both the double well potential (red) and the equivalent gradient term (blue). By construction the gradient energy agrees with the double well term at the 120 deg angle.

$$f_C = \frac{4}{9}\sum_{i<j} |\nabla\phi_i \times \nabla\phi_j|^2. \tag{B.2}$$

For comparison we show the Folch-Plapp potential with the equivalent gradient term in Fig. B.16.

The suggestion here is that just as the potential and gradient term balance, so should the hump function balance with the cross term, Eq. (B.2). However, inclusion of the cross term means having an inconvenient forth order surface energy term.

References

[1] G. Toth, Phase-field modeling of isothermal quasi-incompressible multicomponent liquids, Physica Rev. E 94 (2016) 033114.
[2] R. Folch, M. Plapp, Towards a quantitative phase-field model of two-phase solidification, Phys. Rev. E 68 (2003) 010602.
[3] R. Folch, M. Plapp, Quantitative phase-field modeling of two-phase growth, Phys. Rev. E 72 (2005) 011602.
[4] A. Wheeler, W. Boettinger, G. McFadden, Phase-field model for isothermal phase transitions in binary alloys, Phys. Rev. A 45 (10) (1992) 7424–7440.
[5] P.C. Bollada, P.K. Jimack, A.M. Mullis, Bracket formalism applied to phase field models of alloy solidification, Comput. Mater. Sci. 126 (2017) 426–437.
[6] G.I. Toth, T. Pusztai, L. Granasy, Consistent multiphase-field theory for interface driven multidomain dynamics, Phys. Rev. B 92 (2015) 184105.
[7] M. Plapp, Unified derivation of phase-field models for alloy solidification from a grand-potential functional, Phys. Rev. E 84 (2011) 31601.
[8] P.C. Bollada, P.K. Jimack, A.M. Mullis, Free energy vs. grand potential energy formulations in phase field modelling of alloy solidification, Proceedings of the 7th International Conference on Solidification & Gravity, 2018, pp. 47–51.
[9] A. Karma, W. Rappel, Quantitative phase-field modeling of dendritic growth in two and three dimensions, Phys. Rev. E 57 (4) (1998) 4323–4349.
[10] A.N. Beris, B.J. Edwards, Thermodynamics of Flowing Systems, Oxford University Press, New York, 1994.
[11] O. Penrose, Thermodynamically consistent models of phase-field type for the kinetics of phase transitions, Physica D 43 (1990) 44–62.
[12] B. Nestler, A.A. Wheeler, A multi-phase-field model of eutectic and peritectic alloys: numerical simulation of growth structures, Physica D 138 (2000) 114–133.
[13] P.C. Bollada, P.K. Jimack, A.M. Mullis, A new approach to multi-phase formulation for the solidification of alloys, Physica D 241 (2012) 816–829.
[14] I. Steinbach, A phase field concept for multiphase systems, Physica D 94 (1996) 135–147.
[15] J. Groebner, H.L. Lukas, F. Aldinger, CALPHAD 20 (1996) 2247–2254.
[16] A. Wheeler, W. Boettinger, G. McFadden, Phase-field model of solute trapping during solidification, Phys. Rev. E 47 (3) (1993) 1893–1909.
[17] S.G. Kim, W.T. Kim, T. Suzuki, Phase-field model for binary alloys, Phys. Rev. E 60 (6) (1999) 7186–7197.
[18] A. Karma, Phase-field formulation for quantitative modeling of alloy solidification, Phys. Rev. Lett. 87–11 (2001) 115701.
[19] K. Glasner, Solute trapping and the non-equilibrium phase diagram for solidification of binary alloys, Physica D 151 (2001) 253–270.
[20] B. Echebarria, Quantitative phase-field model of alloy solidification, Phys. Rev. E 70 (2004) 061604.
[21] N. Opoku, A quantitative multi-phase field model of polycrystalline alloy solidification, Acta Mater. 58 (6) (2010) 2155–2164.
[22] Seong Gyoon Kim, Won Tae Kim, Toshio Suzuki, Machiko Ode, J. Crystal Growth 261 (2004) 135–158.
[23] J. Eiken, Multiphase-field approach for multicomponent alloys with extrapolation scheme for numerical application, Phys. Rev. E 73 (2006) 066122.
[24] A. Choudhury, B. Nestler, Grand-potential formulation for multicomponent phase transformations combined with thin-interface asymptotics of the double-obstacle potential, Phys. Rev. E 85 (2012) 21602.
[25] I. Steinbach, L. Zhang, M. Plapp, Phase-field model with finite interface dissipation, Acta Mater. (2012) 2689–2701.
[26] A. Choudhury, M. Kellner, B. Nestler, A method for coupling the phase-field model on a grand-potential formalism to thermodynamic databases, Curr. Opin. Solid State Mater. Sci. 19 (2015) 287–300.
[27] P. Bollada, P.K. Jimack, A.M. Mullis, A numerical approach to compensate for phase field interface effects in alloy solidification, Comput. Mater. Sci. 151 (2018) 338–350.
[28] J. Tiaden, B. Nestler, H.J. Diepers, I. Steinbach, The muiltiphase-field model with an integrated concept for modelling diffusion, Physica D 115 (1998) 73–86.
[29] A. Basak, V.I. Levitas, Nanoscale multiphase phase field approach for stress - and temperature – induced martensitic phase transformations with interfacial stresses at finite points, J. Mech. Phys. Solids 113 (2018) 162–196.
[30] I. Steinbach, F. Pezzolla, A generalized field method for multiphase transformations using interface fields, Physica D 134 (1999) 385–393.
[31] L.Q. Chen, W. Yang, Phys. Rev. B 50 (21) (1994) 15752.
[32] D. Fan, L.-Q. Chen, Acta Mater. 45 (1996) 611–622.
[33] A. Kazaryan, Y. Wang, S. Dregia, B.R. Patton, Grain growth in systems with anisotropic boundary mobility: analytical model and computer simulation, Physica Rev. B 63 (2000) 184102.
[34] N. Moelans, B. Blanpain, P. Wollants, Phys. Rev. B 78 (2008) 024113.
[35] Ofori-Opoku, N. Provatas, A quantitative multi-phase field model of polycrystalline alloy solidification, Acta Mater. 58 (2010) 2155–2164.
[36] M. Gunduz, J.D. Hunt, Acta Metall. 33 (9) (1985) 1651–1672.
[37] M.E. Glicksman, K. Ankit, J. Mater. Sci. 53 (2018) 10955–10978.